ARMA manuscript No.
(will be inserted by the editor)

Thermal creep of a rarefied gas on the basis of non-linear Korteweg-theory

Yong-Jung Kim · Mingi Lee · Marshall Slemrod

Dedicated to the memory of James B. Serrin

Received: November 29, 2013 / Accepted: date

Abstract The study of thermal transpiration or more commonly called thermal creep is accomplished by use of Korteweg's theory of capillarity. Incorporation of this theory into the balance laws of continuum mechanics allows resolution of boundary value problems via solutions to systems of ordinary differential equations. The problem was originally considered by J.C. Maxwell in his classic 1879 paper [29]. In that paper Maxwell derived what is now called the Burnett higher order contribution to the Cauchy stress. But Maxwell was not able to solve his newly derived system of partial differential equations. In this paper the authors note that a more appropriate higher order contribution to the Cauchy stress follows from Korteweg's 1901 theory [23]. The appropriateness of Korteweg's theory is based on the exact summation of the Chapman-Enskog expansion given by A. Gorban and I. Karlin. The resulting balance laws are solved exactly, qualitatively, and numerically and the results are qualitatively similar to the numerical and exact results given by Aoki *et al.*, Loyalka *et al.*, and Struchtrup *et al.*

Keywords gas dynamics · continuum mechanics · thermal creep · thermal transpiration · rarefied gas · Boltzmann equation · Korteweg's theory of capillarity · slip velocity

Mathematics Subject Classification (2000) 76N15 · 74A15

Yong-Jung Kim · Mingi Lee
Department of Mathematical Sciences, KAIST, Daejeon 305-701, Korea
Tel.: +82-42-350-2739, Fax: +82-42-350-2710
E-mail: yongkim@kaist.edu, mg.lee@kaist.ac.kr

Marshall Slemrod (Corresponding author)
Department of Mathematics, University of Wisconsin, Madison, WI 53706, USA
Tel.: +1-608-263-3053, Fax: +1-608-263-8891
E-mail: slemrod@math.wisc.edu

Introduction

The purpose of this paper is to examine the role of Korteweg's theory of capillarity [23] in predicting the steady motion of a rarefied gas where the motion is induced by a temperature gradient on the boundary of the flow domain. The theoretical treatment of problem of such a temperature gradient driven flow dates back to the classical paper of Maxwell [29]. Maxwell noted that he was looking for an explanation to the surface flow phenomena discovered by Kundt and Warburg for gases and Helmholtz and Piotrowski for liquids. Maxwell introduced a linear second gradient of temperature to the Cauchy stress tensor thus realizing that it is the extra contribution to the tangential stress that causes the gas motion adjacent to the domain wall. The velocity of the gas is a slip velocity which Maxwell computed. In equations (55)-(59) of his paper Maxwell derives what he termed the "final equations of motion" and then remarks "I have not, however, attempted to enter into the calculation of the steady motion". Maxwell also remarks "this phenomenon, to which professor Osborne Reynolds has given the name of *thermal transpiration* was discovered entirely by him. He was the first to point out that a phenomenon of this kind was a necessary consequence of the kinetic theory of gases..."

In modern terminology the name thermal transpiration has been replaced by *thermal creep*. More to the point we see from Maxwell's paper that he used the Boltzmann equation (where Maxwell gives full credit to Boltzmann) to derive his higher gradient theory. Hence it is clear that Maxwell in 1879 preceded Hilbert's expansion [7,8,35] (and of course the expansion of Chapman and Enskog [33–35,38,42] and Burnett [5,6]) in deriving a higher order theory of stress from the kinetic theory of gases. In more recent papers Sone and his collaborators [41,42] have continued Maxwell's program and developed a higher order theory of thermal stresses. Furthermore other higher gradient theories are presented in the paper of Lockerby, Reese, and Gallis [25]. Hence, in principle, if one was to use a continuum mechanical approach to thermal creep Sone *et al.*'s expansion [41,42] would provide the equations for the analysis. On the other hand van der Waals [27] in 1894 introduced a variational form of a second gradient theory which was later put in more general form as a stress tensor in 1901 by Korteweg [23]. In recent papers [38–40] the third author of this paper, based on Gorban and Karlin's exact summation of the Chapman-Enskog expansion [15–18,21] for a linearization of Grad's 13 moment expansion [19,20], has suggested that the sum of the Chapman-Enskog expansion has the appearance of Korteweg's theory. In fact for the case of isobaric motion where the product of density and temperature is a constant the theories of Maxwell, Sone *et al.*, Lockerby *et al.*, Bobylev *et al.* [1–4], and Korteweg all appear to be similar at the linear level. But, since Korteweg's theory in the form written by Dunn and Serrin [14] (which was in turn motivated by [36,37]) gives a nonlinear, simple and frame indifferent version of the higher order stress, it is the one we choose to use here.

In the literature on thermal creep one may find two recent themes evolving. The first view is within the context of the kinetic theory of gases. This means

solving the Boltzmann equation or moment approximation to the Boltzmann equations motivated by Grad's 13 moment expansion. Numerically computed solutions of the linearized Boltzmann has been provided by Ohwada *et al.* [30, 31], Loyalka *et al.* [26–28]. Explicit solutions of Struchtrup *et al.*'s regularized 13 moment equations are provided in a series of papers [43–45] (See also the paper of Karlin *et al.* [22] for a further discussion of R13). Inspection of the results given in the paper of Takesi, Rana, Torrilhon, and Struchtrup [45] shows qualitative agreement for their exact solutions and the numerical ones for the linearized Boltzmann equation. The non-numerical papers known to the authors are the works of C.-C.Chen *et al.* [9] and I.-K. Chen *et al.* [10–12, 46] where sharp estimates are obtained on the velocity of the flow in terms of the data and Knudsen number. Again the linear Boltzmann equation is used as the fundamental description for the gas motion. Of course the second theme in the literature is continuum theory as reviewed by Lockerby *et al.* [24,25], and this is the direction we pursue here.

Again we summarize our goal here: we use the non-linear Korteweg theory to allow us to develop sets of non-linear ordinary differential equations for thermal creep flow. Furthermore, for the case of half-plane flow, we give an explicit solution to these nonlinear equations. For channel and wedge flow we give a mixture of qualitative and quantitative results. We believe the material here gives continuation of the issues raised by Lockerby, Reese, and Gallis [25] as to the "usefulness" of higher order constitutive relations in describing rarefied gas flow, i.e., the "usefulness" is allowing non-linear problems in rarefied flow to be represented as systems of non-linear ordinary differential equations which can be analyzed and in some cases explicitly solved. Moreover, to return to our earlier quote from Maxwell's paper: unlike Maxwell, as is obvious from the above remarks, we *do attempt* to give the calculation of non-linear steady motion of the gas.

Contents

1 Balance laws for isobaric flow

The balance laws of mass, momentum, and energy for steady flow in two space dimensions (x, y) are given by

$$\frac{\partial}{\partial x}(\rho u) + \frac{\partial}{\partial y}(\rho v) = 0, \tag{1.1}$$

$$\begin{aligned} &\frac{\partial}{\partial x}(\rho u^2 - T_{11}) + \frac{\partial}{\partial y}(\rho uv - T_{12}) = 0, \\ &\frac{\partial}{\partial x}(\rho uv - T_{12}) + \frac{\partial}{\partial y}(\rho v^2 - T_{22}) = 0, \end{aligned} \tag{1.2}$$

$$\begin{aligned} &\frac{\partial}{\partial x}((e + \frac{1}{2}(u^2 + v^2))\rho u) + \frac{\partial}{\partial y}((e + \frac{1}{2}(u^2 + v^2))\rho v) \\ &\quad = \frac{\partial}{\partial x}(uT_{11} + vT_{12}) + \frac{\partial}{\partial y}(uT_{12} + vT_{22}) - \frac{\partial q_1}{\partial x} - \frac{\partial q_2}{\partial y}. \end{aligned} \tag{1.3}$$

Here we have

ρ	density,
(u, v)	velocity,
T_{ij}	Cauchy stress tensor,
e	specific internal energy,
θ	temperature,
q	heat flux,
p	pressure,
c	capillarity coefficient.

We impose constitutive relations as follows. The Cauchy stress

$$T_{ij} = T^E_{ij} + T^V_{ij} + T^K_{ij},$$

where $T^E_{ij}, T^V_{ij}, T^K_{ij}$ are the elastic, viscous, and Korteweg contributions to the Cauchy stress. Denote $T^{V+K}_{ij} := T^V_{ij} + T^K_{ij}$. We set

$$\begin{aligned} p &= \rho\,\theta, \\ T^E_{ij} &= -p\delta_{ij}, \\ T^V_{ij} &= \lambda(\mathrm{tr}D)\delta_{ij} + 2\mu D_{ij}, \end{aligned}$$

where $\mu > 0$, $\lambda = -\frac{2}{3}\mu$,

$$D_{11} = \frac{\partial u}{\partial x}, \quad D_{12} = D_{21} = \frac{1}{2}(\frac{\partial u}{\partial x} + \frac{\partial v}{\partial y}), \quad D_{22} = \frac{\partial v}{\partial y},$$

and

$$T^K_{ij} = \{\rho c\Delta\rho + \rho c_\rho M + 2\rho c_M d \otimes d \cdot \nabla^2\rho + \rho c_\theta g \cdot d\}\delta_{ij} - cd \otimes d.$$

(Subscripts ρ, θ, M denote partial derivatives with respect to the quantities.) Here, λ, μ are viscosity coefficients of a monatomic gas, $c = c(\rho, \theta, M)$ is the surface tension coefficient, $d = \nabla\rho$, $g = \nabla\theta$ and $M = d \cdot d$ and we choose a system of dependent variables so that the gas constant $R = 1$. The form of T_{ij}^K is taken from the paper of Dunn and Serrin [14]. The internal energy e consists of two parts,

$$e = e^E + e^K,$$

where

$$e^E = \frac{3}{2}\theta$$

is the classical elastic contribution to the internal energy and

$$e^K = \frac{c - \theta c_\theta}{2\rho} d \cdot d$$

is the Korteweg contribution to the internal energy. Finally, the heat flux is given by

$$q = q^F + q^K,$$

where

$$q^F = -\kappa g,$$

is the Fourier contribution to the heat flux and

$$q^K = c\rho \,\mathrm{tr}(D)\nabla\rho$$

is the Korteweg contribution to the heat flux. We take a power law for the capillarity coefficient,

$$c = A\rho^a\theta^b,$$

where a, b are constants. For example, such power law constitutive relations are familiar in the modeling of thermo-mechanical processes (see Tzavaras[47–49]and the extensive references given there).

For comparison, observe Maxwell's second gradient term given in his equation (55) is $\frac{9}{2}\frac{\mu^2}{\rho\theta}\Delta\theta$, which for isobaric flow is proportional to $-\frac{\mu^2}{\rho^2}\Delta\rho+$ nonlinear terms. Maxwell takes $\mu = \mu_0\theta$. This yields $-\mu_0^2\theta^4\Delta\rho$ and with $\rho c = A\rho^{a+1}\theta^b = A\rho^{a-b+1} = A\theta^{b-a-1}$ would require $b-a-1 = 4$, i.e., $b-a = 5$. We note in addition Maxwell's coefficient will be negative, i.e., $-\mu_0^2\theta^4$ where as Korteweg theory gives a positive coefficient. This is no surprise since Maxwell has computed the linear term in Burnett coefficient which we know [2,3] to have the "bad" sign. The point of the papers [38–40] is that the *sum* of the Chapman-Enskog expansion will give the "good" positive sign.

Following Maxwell (see his equation (57)) we consider isobaric flows for which

$$p = 1$$

so that

$$\rho\theta = 1.$$

Isobaric flows will capture the essence of transpiration flow near a solid boundary where there is no induced pressure gradient to drive the flow.

2 Boundary value problems

We consider three boundary value problems: channel flow, half-plane flow, and wedge flow illustrated in Figure 1. We prescribe the following boundary conditions:

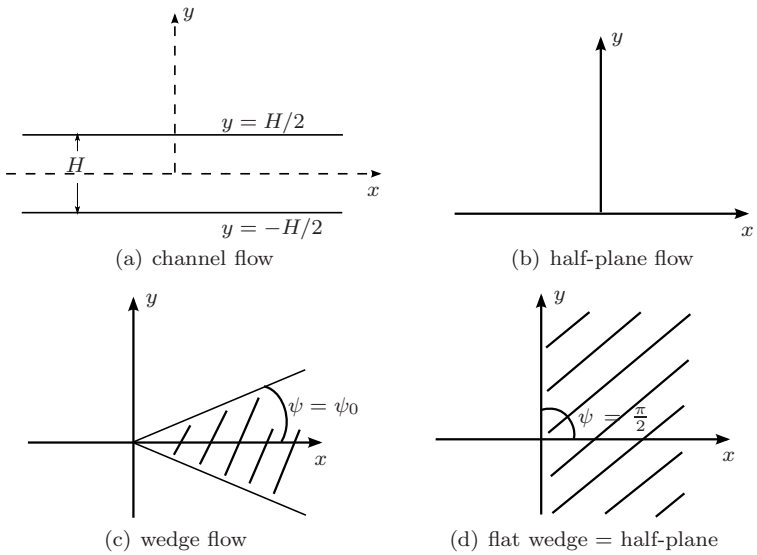

Fig. 1 Three boundary value problems are considered in this paper and their domains are as the above, (a,b) and (c). If the angle $\psi = \frac{\pi}{2}$, the wedge-flow becomes half-plane flow (d).

$$\text{(a) channel:} \quad \theta = \theta_1 |x|^s, \ v(x,y) = 0, \quad |y| = H/2, \tag{2.1}$$

$$\text{(b) half-plane:} \ \theta = \theta_1 |x|^s, \ v(x,y) = 0, \quad y = 0, \tag{2.2}$$

$$\text{(c) wedge:} \quad \theta = \theta_1 r^s, \ (u,v) \cdot \mathbf{n} = 0, \quad \psi = \pm\psi_0, \tag{2.3}$$

where $\mathbf{n} = (-\sin\psi_0, \cos\psi_0)$ is the unit normal vector to the wedge and (r, ψ) is the polar coordinates. Here and in that follows we take a domain $x > 0$ for (a,b) due to the symmetry of the problem with respect to y-axis. We also take the upper half plane $y > 0$ for (c) by the same reason. The power s can be chosen freely and this freedom will be used later to construct a similarity solution in Section 4. Notice that the half-plane flow is a special case of the wedge flow when $\psi_0 = \frac{\pi}{2}$ as demonstrated in (d). The boundary conditions are also identical for these two cases.

Consider a Navier-Stokes-Fourier fluid with

$$\begin{aligned} T_{ij} &= T^E_{ij} + T^V_{ij}, \\ q &= q^F, \\ \kappa &= \kappa_0 \theta^\eta. \end{aligned}$$

Then, $(u, v, \theta) = (0, 0, \Theta)$ will be an exact solution to three isobaric boundary value problems if Θ is the solution of

$$\Delta\Theta^{\eta+1} = 0$$

satisfying the above boundary conditions. In other words, for boundary conditions given by (2.1), (2.2) and (2.3) with the no-slip condition, not only will the Euler equation produce no non-trivial motion but also the Navier-Stokes-Fourier system as well. Since motion is experimentally observed, this points to "incompleteness of continuum fluid dynamics" [25].

3 Rescaled equations for thin layer

We will analyze the isobaric motion in two different ways, one based on a rescaling for motion close to the walls and the second based on self-similarity for which we will recover equations for isobaric motion away from the walls as well.

3.1 Rescaled equations of channel flow

Consider the channel flow problem and set

$$y = \bar{y}H, \quad x = \bar{x}L, \tag{3.1}$$

where L is a typical length scale along the walls. We are interested in the case where

$$\epsilon = \frac{H}{L}$$

is a small parameter. Insertion of (3.1) into (1.1),(1.2),(1.3) immediately yields to leading order in ϵ,

$$\frac{\partial}{\partial\bar{y}}(\rho v) = 0,$$

which incorporated with the boundary condition $v = 0$ on the walls, tells us

$$v \equiv 0.$$

Now (1.2),(1.3) are to leading order,

$$\frac{\partial}{\partial\bar{y}}(T_{12}) = 0, \tag{3.2}$$

$$\frac{\partial}{\partial\bar{y}}(T_{22}) = 0, \tag{3.3}$$

$$\frac{\partial u}{\partial\bar{y}}(T_{12}) - \frac{\partial q_2}{\partial\bar{y}} = 0. \tag{3.4}$$

We look for a solution of the form

$$\begin{aligned} &u = \hat{u}(\bar{y}),\\ &v = 0,\\ &\theta = \bar{x}^s\hat{\theta}(\bar{y}),\\ &\rho = \bar{x}^{-s}\hat{\rho}(\bar{y}),\\ &\hat{\rho}\hat{\theta} = 1, \end{aligned} \tag{3.5}$$

where recall s is determined by the boundary condition (2.1). From (3.5) and the chain rule we find $T^V_{11} = 0,\ T^V_{12} = \mu\frac{\bar{u}'}{H},\ T^V_{22} = 0$ and

$$\begin{aligned} \rho c\Delta\rho &= \frac{\hat{\rho}c}{x^{2s}}\Big(\frac{s(s+1)}{L^2\bar{x}^2}\hat{\rho} + \frac{\hat{\rho}''}{H^2}\Big),\\ \rho c_\rho M &= \frac{\hat{\rho}c_\rho}{\bar{x}^{3s}}\Big(\frac{\hat{\rho}^2}{\bar{x}^2L^2} + \frac{\hat{\rho}'^2}{H^2}\Big),\\ \rho c_\theta g\cdot d &= \frac{\hat{\rho}c_\theta}{\bar{x}^s}\Big(\frac{-s}{\bar{x}^2L^2} - \frac{\hat{\rho}'^2}{\hat{\rho}^2H^2}\Big),\\ -cd\otimes d &= \frac{-c}{\bar{x}^{2s}}\begin{bmatrix} \dfrac{\hat{\rho}^2}{\bar{x}^2L^2} & \dfrac{-\hat{\rho}\hat{\rho}'}{\bar{x}LH}\\[2ex] \dfrac{-\hat{\rho}\hat{\rho}'}{\bar{x}LH} & \dfrac{\hat{\rho}^2}{H^2}\end{bmatrix}. \end{aligned} \tag{3.6}$$

Insert (3.6) into the expression for T^K_{ij} and then read off (to leading order in ϵ) equations (3.2), (3.3),

$$\frac{\partial}{\partial\bar{y}}\Big(\mu\hat{u}' + \frac{c\hat{\rho}\hat{\rho}'}{L\bar{x}^{2s+1}}\Big) = 0 \tag{3.7}$$

and

$$\frac{\partial}{\partial\bar{y}}\Big(\frac{c\hat{\rho}\hat{\rho}''}{\bar{x}^{2s}} + \frac{c_\rho\hat{\rho}\hat{\rho}'^2}{\bar{x}^{3s}} - \frac{c_\theta\hat{\rho}'^2}{\bar{x}^2\hat{\rho}} - \frac{c\hat{\rho}'^2}{\bar{x}^{2s}}\Big) = 0. \tag{3.8}$$

Here, since $c = A\rho^a\theta^b$, c is independent of M and so we set $c_M = 0$.

We have taken $\kappa(\theta) = \kappa_0\theta^\eta$ and hence to have a constant Prandtl number we set $\mu(\theta) = \mu_0\theta^\eta$. Examination of (3.7) tells us to force the same power of $\bar{x}$ in both terms we need

$$\begin{aligned} \mu &= \mu_0\theta^\eta = \mu_0\bar{x}^{s\eta}\hat{\theta}^\eta,\\ \frac{c}{\bar{x}^{2s+1}} = \frac{A\hat{\rho}^{a-b}\bar{x}^{-s(a-b)}}{\bar{x}^{2s+1}} &= A\hat{\rho}^{a-b}\bar{x}^{-s(a-b)-2s-1} \end{aligned}$$

to have the same exponent for $\bar{x}$, i.e.,

$$s\eta = -s(a-b) - 2s - 1.$$

In the rest of this section we set $s = 1$ and hence

$$b - a = \eta + 3. \tag{3.9}$$

For example, for the case of Maxwell molecules, i.e., $\eta = 1$,

$$b - a = 4, \qquad \text{(Maxwell)}$$

and, for hard sphere molecules, $\eta = 1/2$,

$$b - a = \frac{7}{2}. \qquad \text{(Hard Sphere)}$$

If we refer back to Section 1, we see the needed scaling is $b-a = 4$ as opposed to the one predicted by Maxwell himself ($b - a = 5$) from the kinetic theory of gases.

We then see that (3.7) becomes

$$\frac{\partial}{\partial \bar{y}}\Big(\mu_0 \hat{\theta}^{\eta} \hat{u}' + \frac{A\hat{\rho}^{a-b+1}}{L}\hat{\rho}'\Big) = 0$$

or

$$\mu_0 \hat{\theta}^{\eta} \hat{u}' + \frac{A\hat{\rho}^{a-b+1}}{L}\hat{\rho}' = \text{const.} \tag{3.10}$$

We know however that for the channel flow problem the solution $\hat{u}, \hat{\rho}$ should be even in $\bar{y}$ and hence $\hat{u}'(0)$ and $\hat{\rho}'(0)$ must vanish. Thus the constant in (3.10) is zero and with $\hat{\theta}\hat{\rho} = 1$ we have

$$\mu_0 \hat{u}' + \frac{A\hat{\rho}^{a-b+1+\eta}}{L}\hat{\rho}' = 0$$

and integration tells us

$$\mu_0 \hat{u} + \frac{A\hat{\rho}^{a-b+2+\eta}}{L(a-b+2+\eta)} = \text{const.} \tag{3.11}$$

Thus once $\hat{\rho}$ is determined, $\hat{u}$ is known up to two constants.

We must now solve (3.8) subject to the boundary conditions $\hat{\rho} = 1/\theta_1$ at $\bar{y} = \pm 1/2$. Again to get the same power of $\bar{x}$ in each term we need

$$\begin{aligned}
\frac{c}{\bar{x}^{2s}} &= \frac{A\hat{\rho}^{a-b}\bar{x}^{-s(a-b)}}{\bar{x}^{2s}}, \\
\frac{c_\rho}{\bar{x}^{3s}} &= \frac{Aa\hat{\rho}^{a-b-1}\bar{x}^{-s(a-b-1)}}{\bar{x}^{3s}}, \\
\frac{c_\theta}{\bar{x}^{s}} &= \frac{Ab\hat{\rho}^{a-b+1}\bar{x}^{-s(a-b+1)}}{\bar{x}^{s}}
\end{aligned}$$

to have the same exponent for $\bar{x}$, i.e.,

$$-s(a-b) - 2s = -s(a-b-1) - 3s = -s(a-b+1) - s,$$

which is indeed true. Thus (3.8) becomes

$$\frac{\partial}{\partial \bar{y}}\Big(A\hat{\rho}^{a-b+1}\hat{\rho}'' + (Aa\hat{\rho}^{a-b} - Ab\hat{\rho}^{a-b} - A\hat{\rho}^{a-b})\hat{\rho}'^2\Big) = 0 \tag{3.12}$$

or

$$\hat{\rho}\hat{\rho}'' + (a-b-1)\hat{\rho}'^2 = \frac{C_1}{\hat{\rho}^{a-b}}, \tag{3.13}$$

where C_1 is a generic constant. Set

$$w = \hat{\rho}'^2$$

so that $\frac{dw}{d\bar{y}} = 2\hat{\rho}'\hat{\rho}''$. Then, (3.13) becomes

$$\frac{\hat{\rho}\frac{dw}{d\bar{y}}}{2\frac{d\hat{\rho}}{d\bar{y}}} + (a-b-1)w = \frac{C_1}{\hat{\rho}^{a-b}},$$

or

$$\frac{dw}{d\hat{\rho}} + \frac{2(a-b-1)w}{\hat{\rho}} = \frac{2C_1}{\hat{\rho}^{a-b+1}}. \tag{3.14}$$

Equation (3.14) admits the integrating factor $\hat{\rho}^{2(a-b-1)}$. Multiply (3.14) by this integrating factor to obtain

$$\frac{d}{d\hat{\rho}}(\hat{\rho}^{2(a-b-1)}w) = 2C_1\hat{\rho}^{a-b-3},$$

which we integrate to see

$$\hat{\rho}^{2(a-b-1)}w = \frac{2C_1\hat{\rho}^{a-b-2}}{a-b-2} + C_2,$$

where C_2 is also a constant. Hence we have

$$\begin{aligned}\Big(\frac{d\hat{\rho}}{d\bar{y}}\Big)^2 = w &= \frac{2C_1\hat{\rho}^{b-a}}{a-b-2} + C_2\hat{\rho}^{-2(a-b-1)} \\ &= \hat{\rho}^{b-a}\Big(\frac{2C_1}{a-b-2} + C_2\hat{\rho}^{b-a+2}\Big).\end{aligned} \tag{3.15}$$

For $b-a>3$, as in the case of Maxwell molecules and hard sphere molecules, take $C_1>0$, $C_2>0$ so that (3.15) gives us the phase plane portrait in Figure 2 where $\frac{d\hat{\rho}}{d\bar{y}}=0$ when $\frac{2C_1}{a-b-3}+C_2\hat{\rho}^{-a+b+2}=0$. Hence the crossing point on the $\hat{\rho}$ axis moves as we adjust the ratio $\frac{C_1}{C_2}$. We derive the graph given by (3.15) and note the intersection with the vertical line $\hat{\rho}=\frac{1}{\theta_1}$. We desire the travel time between the points of intersection equal to 1, i.e., $-\frac{1}{2}<\bar{y}<\frac{1}{2}$. This is accomplished by adjusting our ratio $\frac{C_1}{C_2}$ since this will monotonically increase travel time from zero as we move the phase portrait to the right. This proves existence of a solution of (3.13) satisfying $\hat{\rho}(\frac{1}{2})=\hat{\rho}(-\frac{1}{2})=\frac{1}{\theta_1}$. Hence we know $\hat{\rho}$ and from (3.11) we know $\hat{u}$ as well. Should we desire an explicit solution to (3.15) we can substitute values of $b-a$, which reduces the problem to a quadrature. For example, $b-a=4$ for Maxwell molecules and,

$$\Big(\frac{d\hat{\rho}}{d\bar{y}}\Big)^2 = \hat{\rho}^4\Big(-\frac{C_1}{3} + C_2\hat{\rho}^6\Big),$$

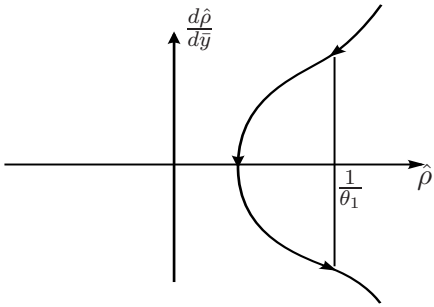

Fig. 2 The phase plane portrait given by (3.15).

$$\frac{1}{\hat{\rho}^2}\Big(C_2\hat{\rho}^6 - \frac{C_1}{3}\Big)^{-\frac{1}{2}}\frac{d\hat{\rho}}{d\bar{y}} = \pm 1;$$

$b - a = \frac{7}{2}$ for hard spheres and,

$$\Big(\frac{d\hat{\rho}}{d\bar{y}}\Big)^2 = \hat{\rho}^{7/2}\Big(-\frac{4C_1}{11} + C_2\hat{\rho}^6\Big),$$

$$\frac{1}{\hat{\rho}^{7/4}}\Big(C_2\hat{\rho}^6 - \frac{4C_1}{11}\Big)^{-\frac{1}{2}}\frac{d\hat{\rho}}{d\bar{y}} = \pm 1.$$

Finally we note that a sketch of the velocity profile is easily obtained from the phase-plane portrait given in Figure 2. Notice that as we move along the trajectory in the figure, say from top to bottom, beginning and ending at $\hat{\rho} = 1/\theta_1$, $\hat{\rho}$ decreases to what would be the value at $\bar{y} = 0$ and then symmetrically increases again. Thus, since the exponent

$$a - b + 2 + \eta$$

in equation (3.11) is negative, it tells us that the profile for $\hat{u}$ will increase, reach a maximum at $\bar{y} = 0$, and then symmetrically decrease. But one easily sees that this is consistent with numerically computed profile given in Figure 8 of [31].

3.2 Rescaled equations of half-plane flow

In our analysis of half-plane flow we anticipate a boundary layer of height H and where again L is a typical length along the wall. Hence the derivation of equations in (3.10) and (3.13) for $\hat{u}$ and $\hat{\rho}$ is exactly the same as for channel flow. In both (3.10) and (3.13) there are constants of integration and we impose the far field conditions

$$\hat{\rho}', \hat{u}' \to 0 \quad \text{as} \quad \bar{y} \to \infty \tag{3.16}$$

that yield these constants to be zero. Hence $\hat{u}$ is once again determined by (3.12) where as $\hat{\rho}$ is given as a solution of

$$\hat{\rho}\hat{\rho}'' + (a-b-1)\hat{\rho}'^2 = 0, \tag{3.17}$$

$$\hat{\rho}(0) = \frac{1}{\theta_1}. \tag{3.18}$$

Division by $\hat{\rho}\hat{\rho}'$ in (3.17) gives

$$\ln \hat{\rho}' + \ln \rho^{a-b-1} = C$$

and allows us to explicitly solve (3.17) and (3.18) to find

$$\hat{\rho}(\bar{y}) = \left(C_3\bar{y} + \left(\frac{1}{\theta_1}\right)^{a-b}\right)^{\frac{1}{a-b}}, \quad C_3 = (a-b)e^C. \tag{3.19}$$

Substitute (3.19) into (3.11) and we can read off the explicit solution for the half-plane problem,

$$\mu_0\hat{u} + \frac{A(C_3\bar{y} + \theta_1^{b-a})^{\frac{a-b+2+\eta}{a-b}}}{L(a-b+2+\eta)} = \text{const}. \tag{3.20}$$

Recall (3.9):

$$b - a = \eta + 3.$$

Hence the exponent in (3.20) is $\frac{1}{4}$ for Maxwell molecules and $\frac{3}{8}$ for hard spheres when $s = 1$. Furthermore the constant C_3 is negative for all cases. Now (3.20) becomes

$$\mu_0\hat{u} - \frac{A}{L}(C_3\bar{y} + \theta_1^4)^{\frac{1}{4}} = \text{const} \tag{3.21}$$

for Maxwell molecules, and

$$\mu_0\hat{u} - \frac{A}{L}(C_3\bar{y} + \theta_1^{\frac{8}{3}})^{\frac{3}{8}} = \text{const} \tag{3.22}$$

for hard spheres. Therefore, the negative sign of C_3 shows that the gas flow moves to left in the domain $x > 0$ if no slip boundary condition is imposed.

We notice that unlike the numeric and analytic results of Ohwada *et al.* [31], Loyalka *et al.* [26–28] and Struchtrup *et al.* [44,45] equation (3.20) gives a (i) sublinear growth of $|\hat{u}|$ in $\bar{y}$ as opposed to a graph of the form (ii) $\hat{u} = \text{const}_0 + \sum_{i\geq 1} \text{const}_i \exp(-\beta_i\bar{y})$ when $\beta_i > 0$. The reason for (ii) is an immediate result of their model. The authors use a *linear* model and as is well known from the theory of constant coefficient evolution equations, if there are no oscillations (damped or undamped), then all bounded solutions must be of the form (ii). Hence, there is no inconsistency between (i) and (ii). Both provide the magnitude of $\hat{u}$ as a monotone increasing, concave function of $\bar{y}$. One might question the growth of $\hat{u}$ for large $\bar{y}$. But of course once $\bar{y}$ becomes large (say of order $\frac{1}{\epsilon}$), then the original scaling arguments used to derive the ordinary differential equation for $\hat{u}$ and $\hat{\rho}$ are no longer valid. This motivates deriving a system of ordinary differential equations where the scaling in ϵ is

not used and we shall do this in the next section. Finally, in both Sections 3.1 and 3.2, we have $\frac{\partial q_2}{\partial \bar{y}} = 0$.

If we wish to compute q_1, we note that since q_1^K is zero to leading order in ϵ, the dominant term is given by q_1^F which for the half-plane flow yields

$$\begin{aligned} q_1^F &= -\kappa(\theta)\frac{\partial \theta}{\partial x} = \frac{-\kappa_0 s \hat{\theta}^{\eta+1}}{L} = \frac{-\kappa_0 s \hat{\rho}^{-(\eta+1)}}{L} \\ &= \frac{-\kappa_0 s}{L}(C_3 \bar{y} + \theta_1^{b-a})^{\frac{\eta+1}{b-a}}, \end{aligned}$$

which again gives exponents $\frac{1}{2}$ for Maxwell molecules and $\frac{3}{8}$ for hard spheres and hence gives sublinear growth in $\bar{y}$.

4 Self-similar solutions for flows over a wedge

As noted in Section 3.2 the result derived from Korteweg theory given by (3.20) will become inconsistent with their derivation for large y where as the results of Loyalka *et al.*, Struchtrup *et al.*, and Ohwada *et al.* [31] will inevitably reflect the linearity assumption of their underlying systems of equations. This motivates us to derive a system of ordinary differential equations for isobaric flow not based on the smallness of y or linearity.

It is well-known that the conservation laws given in (1.1)–(1.3) have the similarity structure along a variable $\xi = \frac{y}{x}$. Therefore, we may consider a similarity solution in terms of polar coordinates. First, we rewrite the conservation laws in polar coordinates r and ψ. The velocity vector field is written as

$$(u, v) = w_1 \mathbf{e}_r + w_2 \mathbf{e}_\psi = (w_1, w_2)_\wp (\equiv \mathbf{w}),$$

where $\mathbf{e}_r = (\cos\psi, \sin\psi)$ and $\mathbf{e}_\psi = (-\sin\psi, \cos\psi)$ are unit vectors in polar coordinate system and the subscript '$\wp$' in $(w_1, w_2)_\wp$ is to denote this coordinate system. The stress tensors are written as

$$\begin{aligned} T_{ij}^E &= -p\delta_{ij} \\ T^V &= \mu \begin{pmatrix} 2\frac{\partial w_1}{\partial r} - \frac{2}{3}\nabla\cdot\mathbf{w} & \frac{1}{r}\frac{\partial w_1}{\partial \psi} + \frac{\partial w_2}{\partial r} - \frac{w_2}{r} \\ \frac{1}{r}\frac{\partial w_1}{\partial \psi} + \frac{\partial w_2}{\partial r} - \frac{w_2}{r} & 2\Big(\frac{1}{r}\frac{\partial w_2}{\partial \psi} + \frac{w_1}{r}\Big) - \frac{2}{3}\nabla\cdot\mathbf{w} \end{pmatrix} \\ T_{ij}^K &= \rho\nabla\cdot\big(c(\rho,\theta)\nabla\rho\big)\delta_{ij} - c(\rho,\theta)\nabla\rho\otimes\nabla\rho. \end{aligned}$$

The mass conservation (1.1) is written as

$$\nabla\cdot(\rho\mathbf{w}) = \frac{1}{r}\frac{\partial}{\partial r}(r\rho w_1) + \frac{1}{r}\frac{\partial(\rho w_2)}{\partial \psi} = 0. \tag{4.1}$$

The momentum conservation (1.2) is written as

$$\nabla\cdot S = \begin{pmatrix} \frac{1}{r}\Big(\frac{\partial}{\partial r}(rS_{11})\Big) + \frac{1}{r}(\frac{\partial}{\partial \psi}S_{12} - S_{22}) \\ \frac{1}{r}\Big(\frac{\partial}{\partial r}(rS_{12})\Big) + \frac{1}{r}(\frac{\partial}{\partial \psi}S_{22} + S_{12}) \end{pmatrix} = 0, \tag{4.2}$$

where S is a symmetric tensor given by

$$S = \rho \mathbf{w} \otimes \mathbf{w} - T^{V+K}.$$

Now, we will construct a special solution in a form of

$$\begin{array}{rl} \rho & = r^{\alpha} \ \tilde{\rho}(\psi), \\ w_1 & = r^{\gamma} \ \tilde{w}_1(\psi), \\ w_2 & = r^{\gamma} \ \tilde{w}_2(\psi), \\ \theta & = r^{\beta} \ \tilde{\theta}(\psi), \\ T_{ij}^{V+K} & = r^{\delta} \ \tilde{T}_{ij}(\psi), \end{array} \tag{4.3}$$

and $\tilde{\rho}\tilde{\theta} = 1$. The powers are given by

$$\alpha = \frac{-1}{2\eta+1}, \quad \beta = \frac{1}{2\eta+1}, \quad \gamma = \frac{-\eta}{2\eta+1}, \quad \delta = -1, \tag{4.4}$$

where

$$\mu = \mu_0 \theta^{\eta}, \quad c(\rho, \theta) = A\rho^a \theta^b = A\theta^{b-a}$$

and

$$b - a = 3 + 2\eta. \tag{4.5}$$

The choice of the powers above are from similarity structure of the problem, which is briefly discussed in the Appendix. In particular, notice the difference from the previous choice in (3.9).

The first step is to find equations for $\tilde{\rho}, \tilde{\theta}, \tilde{T}_{ij}$, and $\tilde{\mathbf{w}} := (\tilde{w}_1, \tilde{w}_2)_{\wp}$ by substitution of the ones in (4.3) into the balance of mass and momentum. First the mass flux is written as

$$\rho \mathbf{w} = r^{\alpha+\gamma} \tilde{\rho} \tilde{\mathbf{w}}.$$

Hence, the mass conservation, $\nabla \cdot (\rho \mathbf{w}) = 0$, is written as

$$(\alpha + \gamma + 1)\tilde{\rho}\tilde{w}_1 + (\tilde{\rho}\tilde{w}_2)' = 0, \tag{4.6}$$

where the ordinary differentiation above is with respect to ψ variable.

There are three tensors for momentum conservation. Similar substitutions give

$$\rho \mathbf{w} \otimes \mathbf{w} = r^{\alpha+2\gamma} \tilde{\rho} \tilde{\mathbf{w}} \otimes \tilde{\mathbf{w}}, \tag{4.7}$$

$$T^V = r^{\beta\eta+\gamma-1} \tilde{T}^V,$$

$$\tilde{T}^V = \mu_0 \tilde{\theta}^{\eta} \begin{pmatrix} \frac{4\gamma-2}{3}\tilde{w}_1 - \frac{2}{3}(\tilde{w}_2)' & (\tilde{w}_1)' + (\gamma-1)\tilde{w}_2 \\ (\tilde{w}_1)' + (\gamma-1)\tilde{w}_2 & \frac{-2\gamma+4}{3}\tilde{w}_1 + \frac{4}{3}(\tilde{w}_2)' \end{pmatrix}, \tag{4.8}$$

$$T^K = r^{\beta(b-a-2)-2} \tilde{T}^K, \quad \tilde{T}^K = A\tilde{\rho}^{a-b}\big(\beta^2(1-(b-a))\tilde{\rho}^2 +$$

$$\big(\tilde{\rho}\tilde{\rho}'' + (a-b)(\tilde{\rho}')^2\big)\big)\delta_{ij} + A\tilde{\rho}^{a-b} \begin{pmatrix} -\beta^2\tilde{\rho}^2 & \beta\tilde{\rho}\tilde{\rho}' \\ \beta\tilde{\rho}\tilde{\rho}' & -\tilde{\rho}'^2 \end{pmatrix}. \tag{4.9}$$

The powers in (4.4) give

$$\alpha + 2\gamma = \beta\eta + \gamma - 1 = \beta(b-a-2) - 2 = -1 = \delta.$$

Therefore, the tensor S satisfies $S = r^{-1}\tilde{S}$ with

$$\tilde{S} = \tilde{\rho}\tilde{\mathbf{w}} \otimes \tilde{\mathbf{w}} - \tilde{T}^V - \tilde{T}^K.$$

The momentum conservation is written as

$$\nabla \cdot S = 0 \Rightarrow \begin{pmatrix} (1+\delta)\tilde{S}_{11} + \tilde{S}'_{12} - \tilde{S}_{22} \\ (1+\delta)\tilde{S}_{12} + \tilde{S}'_{22} + \tilde{S}_{12} \end{pmatrix} = \begin{pmatrix} \tilde{S}'_{12} - \tilde{S}_{22} \\ \tilde{S}'_{22} + \tilde{S}_{12} \end{pmatrix} = 0. \tag{4.10}$$

(Notice that the above choice of the power $\delta = -1$ simplifies the momentum conservation.) Therefore,

$$\tilde{S}''_{12} + \tilde{S}_{12} = 0, \quad \tilde{S}_{22} = \tilde{S}'_{12},$$

and hence we obtain

$$\begin{aligned} \tilde{S}_{12} &= C_1 \cos\psi + C_2 \sin\psi \\ &= \tilde{\rho}\tilde{w}_1\tilde{w}_2 - \mu_0\tilde{\rho}^{-\eta}(\tilde{w}'_1 + (\gamma-1)\tilde{w}_2) - A\beta\tilde{\rho}^{a-b+1}\tilde{\rho}', \qquad (4.11) \\ \tilde{S}_{22} &= -C_1 \sin\psi + C_2 \cos\psi = \tilde{\rho}\tilde{w}_2^2 - \mu_0\tilde{\rho}^{-\eta}\Big(\frac{4}{3}\tilde{w}'_2 + \frac{4-2\gamma}{3}\tilde{w}_1\Big) \\ &\quad -A\tilde{\rho}^{a-b}((1+a-b)\beta^2\tilde{\rho}^2 + \tilde{\rho}\tilde{\rho}'' + (a-b+1)\tilde{\rho}'^2 - 2\tilde{\rho}'^2). \qquad (4.12) \end{aligned}$$

Notice that we do not consider the equation for energy conservation. The reason for this is both mathematical and physical. Of course the mathematical basis for ignoring energy conservation is obvious: (4.6), (4.11) and (4.12) will provide a closed system of ordinary differential equations in $\tilde{\rho}, \tilde{w}_1$ and $\tilde{w}_2$. The physical basis for neglecting energy balance may be found in the paper of Sone where he writes on the discrepancy of the Navier-Stokes system [41, Section 3.1]. "Anyway, the heat-conduction equation is not appropriate to the description of the temperature field of the problem ... the temperature field has to be obtained simultaneously with the flow with the case of the continuity and momentum equations." Sone bases his remarks on order of magnitude relations in the balance laws. Mathematically the energy equation would have to be modified by the terms q_1^K, q_2^K and e^K. Now just as in the more traditional examples of isothermal and isentropic gas dynamics in absence of the heat flux the balance of mass and momentum will imply the energy *equality*. This is of course familiar in continuum thermodynamics (see C.M. Dafermos [13]). Moreover, it is interesting to note that Maxwell himself weighed in on this issue. He wrote "However, it is important this consideration may be in the theory of specific heat and that of conduction of heat, it has only a secondary bearing on the question of stresses in the medium; and as it would introduce great complexity and much guess-work into our calculations..."

4.1 Numerical computation of the similarity equations

The three equations in (4.6), (4.11) and (4.12), make a system that involves first order derivatives of $\tilde{w}_1$ and $\tilde{w}_2$ and first and second order derivatives of $\tilde{\rho}$. Hence, we obtain first order system of four equations

$$\tilde{\rho}' = \tilde{\omega}, \tag{4.13}$$

$$\tilde{w}_1' = (1-\gamma)\tilde{w}_2 - \frac{A\beta}{\mu_0}\tilde{\rho}^{-\eta-2}\tilde{\omega} + \frac{\tilde{\rho}^{\eta}}{\mu_0}(\tilde{\rho}\tilde{w}_1\tilde{w}_2 - C_1\cos\psi - C_2\sin\psi), \tag{4.14}$$

$$\tilde{w}_2' = -(\alpha+\gamma+1)\tilde{w}_1 - \frac{\tilde{\omega}}{\tilde{\rho}}\tilde{w}_2, \tag{4.15}$$

$$\tilde{\omega}' = \tilde{\rho}^{-1}((b-a-1)(\beta^2\tilde{\rho}^2+\tilde{\omega}^2)+2\tilde{\omega}^2) + \frac{1}{A}\tilde{\rho}^{b-a}\tilde{w}_2^2 - \frac{\tilde{\rho}^{b-a-1}}{A}\times \Big(C_2\cos\psi - C_1\sin\psi + \mu_0\tilde{\rho}^{-\eta}((\frac{4}{3}\beta-2\gamma)\tilde{w}_1 - \frac{4\tilde{\omega}}{3\tilde{\rho}}\tilde{w}_2)\Big). \tag{4.16}$$

We solve this problem on an interval $[\psi_0, \pi]$ with initial conditions

$$\tilde{\rho}(\psi_0) = \tilde{\rho}_0 > 0,\ \tilde{w}_1(\psi_0) = \tilde{w}_{10},\ \tilde{w}_2(\psi_0) = 0,\ \tilde{\omega}(\psi_0) = \tilde{\omega}_0, \tag{4.17}$$

where ψ_0 is the angle of wedge. Note that the above C_1 and C_2 are not arbitrary constants. They have to be chosen appropriately. For example, the angular component of the velocity vector should be zero at the other side of the wedge, i.e.,

$$\tilde{w}_2(2\pi - \psi_0) = 0. \tag{4.18}$$

Notice that we consider a symmetric wedge and hence a symmetric solution with respect to x-axis. Therefore, the constants C_1 and C_2 should be chosen to satisfy

$$\tilde{w}_2(\pi) = 0. \tag{4.19}$$

In the numerical examples and computations of this section C_1 and C_2 were chosen in a way that (4.19) is satisfied. The existence of such C_1 and C_2 seems to depend on the initial values in (4.17) and the wedge angle ψ_0. We could not show existence or uniqueness of such constants that give the symmetry to a solution.

In Figure 3 the velocity vector fields of four similarity solutions are given in xy-plane. In these examples, hard sphere case is considered with $\eta = 1$. Two cases of wedge angles are considered with $\psi_0 = 0, \pi/6$, where $\psi_0 = 0$ should be considered as the limiting case that the wedge angle approaches to zero. Since the power $\gamma < 0$, the far field velocity is zero. However, to generate these flow under the isobaric assumptions, the temperature diverges as $r \to \infty$ since $\beta > 0$ and the gas is a vacuum at the far field. The examples in Figures 3(a,c) are with slip boundary conditions and in Figures 3(b,d) are with no slip boundary condition. In particular Figures 3(b,d) show that the similarity solution is not stationary even if the velocity field is zero along the wedge.

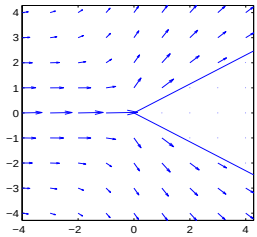

(a) slip boundary condition with $\psi_0 = \frac{\pi}{6}$

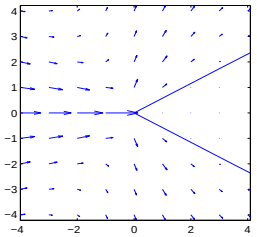

(b) no slip condition with $\psi_0 = \frac{\pi}{6}$

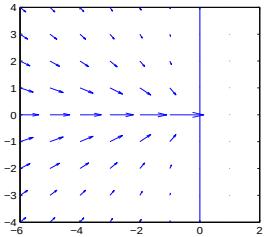

(c) no slip condition with $\psi_0 = \frac{\pi}{2}$

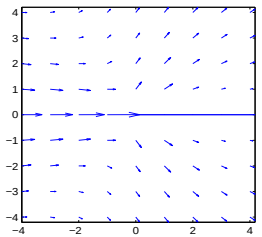

(d) no slip condition with $\psi_0 = 0$

Fig. 3 Velocity vector fields of similarity solutions for wedge problem (4.13)–(4.19) in xy-plane. Slip boundary condition $\tilde{w}_1(\psi_0) = 1$ is given for (a), and no slip boundary condition $\tilde{w}_1(\psi_0) = 0$ is given for (b,c,d). The wedge angle is $\psi_0 = \pi/6$ for (a), $\psi_0 = \frac{\pi}{2}$ for (b), and $\psi_0 = 0$ for (c,d). The other boundary conditions are identical with $\tilde{w}_2(\psi_0) = 0$, $\tilde{\rho}(\psi_0) = 1$ and $\rho'(\psi_0) = 0$ and constants C_1 and C_2 have been chosen to satisfy $\tilde{w}_2(\pi) = 0$.

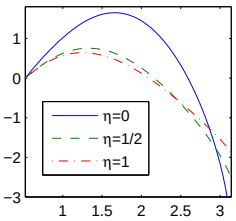

(a) $\tilde{w}_1(\psi)$

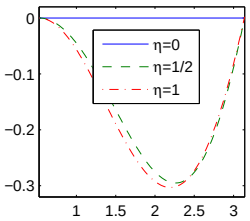

(b) $\tilde{w}_2(\psi)$

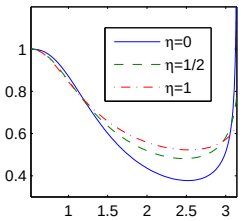

(c) $\tilde{\rho}(\psi)$

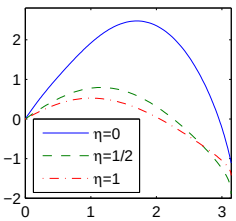

(d) $\tilde{w}_1(\psi)$

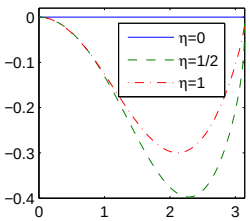

(e) $\tilde{w}_2(\psi)$

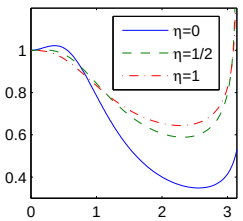

(f) $\tilde{\rho}(\psi)$

Fig. 4 [horizontal-axis: angle ψ]. Similarity solution of (4.13)–(4.18) with no slip boundary condition. The first row is the case in Figure 3(b) with $\psi_0 = \pi/6$ and the second row is in Figure 3(d) with $\psi_0 = 0$. Three cases of $\eta = 0, 0.5, 1$ are considered.

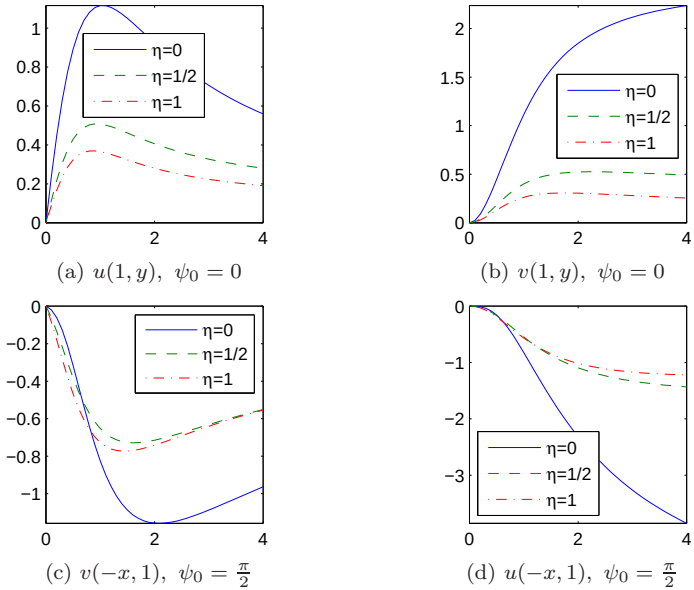

(a) $u(1,y),\ \psi_0 = 0$ (b) $v(1,y),\ \psi_0 = 0$

(c) $v(-x,1),\ \psi_0 = \frac{\pi}{2}$ (d) $u(-x,1),\ \psi_0 = \frac{\pi}{2}$

Fig. 5 [horizontal-axis: distance from the horizontal surface.] Velocity vector fields of similarity solution in rectangular xy-coordinates for a thin wedge are given in (a,b). The initial conditions are identical to the case in Figure 3(d) with no slip boundary condition. The half-plane case with the wedge angle $\psi_0 = \frac{\pi}{2}$ as in Figure 1(d) is given in (c,d).

In Figure 4 the profiles of velocity $\tilde{\mathbf{w}} = (\tilde{w}_1, \tilde{w}_2)_{\wp}$ and the density $\tilde{\rho}$ are given for the two cases with no slip boundary conditions. The first row corresponds to the case in Figure 3(b), where three cases of $\eta = 0, 0.5$ and 1 are displayed. The second row is the case in Figure 3(d). In these examples, we have $\tilde{\rho} > 0$ and $\tilde{w}_2 = 0$ for $\eta = 0$ case. These observation will be proved in Theorem 1. In these examples, one may also observe that $\tilde{\rho}$ has a unique local minimum in the interval $[\psi_0, \pi]$. Part of such behavior is shown in Theorem 2.

In Figure 5(a,b), velocity vector fields are given in rectangular coordinates along a line $x = 1$ with $0 < y < 6$. These figures correspond to the case in Figure 3(d) with no slip boundary condition. One may observe the dynamics of the velocity field away from the horizontal thin wedge plate with wedge angle $\psi_0 = 0$. In Figure 5(c,d), velocity vector fields are given similarly for the case with $\psi_0 = \frac{\pi}{2}$. This is the flat wedge in Figure 1(d) that gives the half-plane flow in Section 3.2. The specification of the simulation is same as Figure 3(c). One may observe differences between this half-plane flow and the previous thin wedge plate flow. First notice that the parallel component v to the surface in (c) has the negative sign. This is the same sign obtained from (3.22), where C_3 in the formula is negative. The vertical component u in (d) has zero slope on the boundary and hence is smaller than the horizontal component near the surface. These two components become compatible beyond the thin layer near the surface.

Some of the simulation results agree with other linear theory results. For example, the magnitude of the horizontal component of velocity increases in the thin layer of the plate, say $0 < x < 1$, and approaches to a maximum, which agrees with the results in [45, Figure 6]. However, as x increases beyond the thin layer, the velocity v decreases and converges to zero eventually. This second part shows the difference of the nonlinear theory of this paper from the linear theory.

4.2 The structure of similarity solutions

In this section properties of previously obtained similarity solutions are studied. We have observed several solution structures from numerical computations in the previous section. For example, the gas density $\tilde{\rho}$ was positive and there were at most two critical points in the interval $[0, \pi]$. The angular velocity was identically zero $\tilde{w}_2 = 0$ for the case with $\eta = 0$. We will show some of these observations for the case of $\eta = 0$. We assume the wedge is symmetric and hence the solution is also symmetric with respect to x-axis. Therefore, the range of the angle of our interest is $\psi_0 \le \psi \le \pi$. If $\eta = 0$, the powers in (4.4) become

$$\alpha = -1, \quad \beta = 1, \quad \gamma = 0, \quad \delta = -1, \quad b - a = 3. \tag{4.20}$$

For this case, we can reduce the system for similarity solutions to a single second order ODE of ρ. First the conservation of mass, (4.6), is written as

$$\big(\tilde{\rho}\tilde{w}_2\big)' = 0 \quad \Rightarrow \quad \tilde{\rho}\tilde{w}_2 = \text{const.}$$

Since $\tilde{w}_2(\psi_0) = 0$, this constant should be zero. Therefore, if the gas density $\rho(\psi)$ is positive on an interval $[\psi_0, \tau]$, then the angular velocity is zero in the interval, i.e.,

$$\tilde{w}_2(\psi) = 0, \quad \psi_0 < \psi < \tau. \tag{4.21}$$

One may observe this phenomenon from Figures 4(b) and (e). In the followings, we will show that we may take $\tau = \pi$ unless the solution blows up.

The equations (4.11) and (4.12) are simplified as

$$C_1 \cos\psi + C_2 \sin\psi = -\mu_0 \tilde{w}_1' - A\tilde{\rho}^{-2}\tilde{\rho}', \tag{4.11}'$$

$$-C_1 \sin\psi + C_2 \cos\psi = -\mu_0\Big(\frac{4}{3}\tilde{w}_1\Big) - A\tilde{\rho}^{-3}(-2\tilde{\rho}^2 + \tilde{\rho}\tilde{\rho}'' - 4\tilde{\rho}'^2). \tag{4.12}'$$

The integration of (4.11)′ gives

$$-\mu_0\tilde{w}_1 = -A\frac{1}{\tilde{\rho}} + C_1 \sin\psi - C_2 \cos\psi + C_3,$$

where C_3 is decided by initial values, i.e.,

$$C_3 = -\mu_0\tilde{w}_1(\psi_0) + A\frac{1}{\tilde{\rho}(\psi_0)} - C_1 \sin\psi_0 + C_2 \cos\psi_0.$$

The substitution of $\mu_0\tilde{w}_1$ into $(4.12)'$ gives

$$\tilde{\rho}'' = 4\frac{(\tilde{\rho}')^2}{\tilde{\rho}} + \frac{2}{3}\tilde{\rho} - \frac{\tilde{\rho}^2}{A}\left(-\frac{7}{3}C_1\sin\psi + \frac{7}{3}C_2\cos\psi - \frac{4}{3}C_3\right). \tag{4.22}$$

Let $z = \tilde{\theta}^3 = \tilde{\rho}^{-3}$. Then, Eq. (4.22) is written as

$$z'' + 2z = \frac{1}{A}\left(-7C_1\sin\psi + 7C_2\cos\psi - 4C_3\right) z^{2/3}.$$

Let

$$R(\psi) := \frac{1}{A}(-7C_1\sin\psi + 7C_2\cos\psi - 4C_3) = B_1\cos(\psi - \bar{\psi}) + B_2, \tag{4.23}$$

where

$$B_1 = \frac{7}{A}\sqrt{C_1^2 + C_2^2} > 0, \quad B_2 = -\frac{4}{A}C_3, \ \bar{\psi} = \tan^{-1}\big(-\frac{C_1}{C_2}\big).$$

Then, z satisfies

$$z'' + 2z = R(\psi)z^{2/3}. \tag{4.24}$$

(Above notations are reserved and appear in the rest of paper.)

Theorem 1 *Let α, β, γ, δ, a and b be given by (4.20) and $\eta = 0$. Then, $\tilde{\rho}(\psi) > 0$ and $\tilde{w}_2(\psi) = 0$ as long as $\tilde{\rho}$ is bounded.*

Proof Let $\tau > \psi_0$ be the first point such that $\rho(\tau) = 0$. Then, $z := \tilde{\rho}^{-3} = \tilde{\theta}^3$ is well defined for $\psi_0 < \psi < \tau$ and satisfies

$$z'' + \Big(2 - \tilde{\rho}R(\psi)\Big)z = 0.$$

Density $\tilde{\rho}$ is bounded on $[\psi_0, \tau) \subset [0, \pi]$ and thus all the coefficients of the second order differential equation are bounded. Therefore z is bounded in $[\psi_0, \tau)$ which contradicts the assumption $\tilde{\rho}(\tau) = 0$. Therefore $\tilde{\rho} > 0$ for all $\psi > \psi_0$ as long as $\tilde{\rho}$ is defined. The same $\tau > \psi_0$ in (4.21) can be any angle in the domain that $\tilde{\rho}$ is bounded and hence the second part of the theorem holds. □

As discussed in previous sections, the global existence of a similarity solution requires $\tilde{w}_2(\pi) = 0$. The theorem guarantees the relation for the case $\eta = 0$ as long as the density $\tilde{\rho}$ is bounded. However, the density may blow up within the interval $\psi \in (\psi_0, \pi]$ depending on the choice of coefficients C_1 and C_2. The following lemma provides a necessary condition for the global existence of a similarity solution.

Lemma 1 *Let α, β, γ, δ, a and b be given by (4.20) and $\eta = 0$. If $R(\psi) \le 0$ in $[a_1, a_2]$, the gas density $\tilde{\rho}$ has no local maximum in $[a_1, a_2]$ and, furthermore, if $a_2 - a_1 \ge \frac{\pi}{\sqrt{2}}$, there exists a blow up angle $\psi_b \in (a_1, a_2)$.*

Proof Let $z_1 := \tilde{\rho}^{-3} = \tilde{\theta}^3$. Since $R(\psi) \le 0$ in the interval $[a_1, a_2]$, we have

$$z_1'' + 2z_1 = R(\psi) z_1^{2/3} \le 0, \quad \psi \in [a_1, a_2]. \tag{4.25}$$

Therefore, by the maximum principle, z_1 has no positive local minimum, i.e., $\tilde{\rho}$ has no positive local maximum. Now we assume $a_2 - a_1 \ge \frac{\pi}{\sqrt{2}}$ and compare z_1 to

$$z_2(\psi) := z_1(a_1)\cos(\sqrt{2}(\psi - a_1)) + \frac{z_1'(a_1)}{\sqrt{2}}\sin(\sqrt{2}(\psi - a_1)),$$

which satisfies $z_2'' + 2z_2 = 0$, $z_2(a_1) = z_1(a_1)$ and $z_2'(a_1) = z_1'(a_1)$. We employ a maximum principle [32, Theorem 14 of Chap.1] and conclude that $z_2 \ge z_1$ on (a_1, a_2) (see Appendix). Now z_2 attains a zero ψ_1 such that

$$\tan(\sqrt{2}(\psi_1 - a_1)) = -\sqrt{2}\frac{z_1(a_1)}{z_1'(a_1)}. \tag{4.26}$$

Since the period of the function '$\tan(\sqrt{2}\,\psi)$' is $\frac{\pi}{\sqrt{2}}$ and $a_2 - a_1 \ge \frac{\pi}{\sqrt{2}}$, there exists $\psi_1 \in (a_1, a_2)$ that satisfies (4.26), i.e., $z_2(\psi_1) = 0$. Since $z_1 \le z_2$ on (a_1, a_2), there exists $\psi_b \in [a, \psi_1]$ such that $\lim_{\psi \to \psi_b} z_1(\psi) = 0$. Therefore, $\lim_{\psi \to \psi_b} \tilde{\rho}(\psi) = \infty$. □

Notice that even if $a_2 - a_1 < \frac{\pi}{\sqrt{2}}$, the solution may blow up depending on the values of $z_1(a_1)$ and $z_1'(a_1)$. Hence the above lemma only gives a necessary condition for the global existence of similarity solution. The choices of C_1 and C_2, together with initial conditions, decide the negative regions of $R(\psi)$. Hence, to expect a similarity solution, one should choose C_1 and C_2 in a way that $R(\psi)$ has positive values in a larger region. On the other hand, similarity solutions have been constructed numerically for all the test cases with $\psi_0 > 0$. Hence it can be conjectured that for any given initial value in (4.17) and wedge angle $\psi_0 > 0$, there exists C_1 and C_2 that gives the global existence of the similarity solution. However, we do not have its proof.

Next we consider the number of critical points of similarity solution.

Lemma 2 *Let α, β, γ, δ, a and b be given by (4.20) and $\eta = 0$. If $R(\psi) \ge 0$ in $[\bar{\psi}, \bar{\psi} + \tau] \subset [0, \pi]$, $\tilde{\theta}$ has a local maximum at $\psi_1 \in [\bar{\psi}, \bar{\psi} + \tau]$, and $\bar{\psi} + \tau - \psi_1 < \frac{\pi}{\sqrt{2}}$, then there is no local minimum in the interval $(\psi_1, \bar{\psi} + \tau)$.*

Proof The proof is similar to the one for Lemma 1. This time we let $z_1 := \frac{d}{d\psi}\tilde{\theta}^3$, which is the derivative of the z_1 in Lemma 1. Then from (4.25), we have

$$z_1'' + \Big(2 - \frac{2}{3}R(\psi)\tilde{\rho}\Big)z_1 = R'(\psi)\tilde{\rho}^{-2} = -B_1 \sin(\psi - \bar{\psi})\tilde{\rho}^{-2} \le 0$$

for $\psi \in [\bar{\psi}, \bar{\psi} + \tau]$. Since ψ_1 is a local maximum of $\tilde{\theta}$, we have $z_1(\psi_1) = 0$ and $z_1'(\psi_1) \le 0$. One may easily check that any z_1 cannot be constant on $(\psi_1, \psi_1 + \epsilon)$ for any $\epsilon > 0$ and hence $z_1'(\psi) < 0$ on $(\psi_1, \psi_1 + \epsilon)$ for a small $\epsilon > 0$.

Hence we may assume $z_1'(\psi_1) > 0$ by taking a slightly larger angle if needed. Now compare z_1 to

$$z_2(\psi) := -\tilde{\epsilon}\sin(\sqrt{2}(\psi - \psi_1)),$$

which satisfies $z_2'' + 2z_2 = 0$ and $z_2(\psi_1) = 0$. By choosing a small $\tilde{\epsilon}$, we have $0 > z_2'(\psi_1) \geq z_1'(\psi_1)$. Furthermore, since $z_2 \leq 0$ and $R \geq 0$ on $[\psi_1, \psi_1 + \frac{\pi}{\sqrt{2}}]$,

$$z_2'' + \Big(2 - \frac{2}{3}R(\psi)\bar{\rho}\Big)z_2 \geq z_2'' + 2z_2 = 0.$$

We employ the maximum principle [32, Theorem 14 of Chap.1] again and conclude that $z_2 \geq z_1$ on $(\psi_1, \bar{\psi}+\tau)$ (see Appendix). However, since $\bar{\psi}+\tau-\psi_1 < \frac{\pi}{\sqrt{2}}$, $z_2 < 0$ on $(\psi_1, \bar{\psi}+\tau)$ and so is z_1. Therefore, $\tilde{\theta}$ has no critical point in the interval. □

Lemma 2 lets us control oscillation behavior in the region $\psi > \bar{\psi}$. Hence we first set $\bar{\psi} = \psi_0$ by fixing the ratio $\frac{C_1}{C_2}$ as

$$\bar{\psi} = \tan^{-1}(-\frac{C_1}{C_2}) = \psi_0, \quad \text{i.e.,} \quad C_1 = -C_2\tan(\psi_0). \tag{4.27}$$

Hence we have one degree of freedom left in choosing the constants. The function $R(\psi)$ is given by

$$R(\psi) = B_1\cos(\psi - \psi_0) + B_2.$$

Since there should be a local maximum between two local minima, the distance between two local minima should be larger than $\frac{\pi}{\sqrt{2}}$.

From the numerical simulations of previous section we have observed that there is at most one local minimum of $\tilde{\rho}$ and $\tilde{\theta}$ in the interval (ψ_0, π). Using the previous two lemmas we show in the following theorem that a similarity solution may have at most two local minima on (ψ_0, π).

Theorem 2 *Let α, β, γ, δ, a and b be given by (4.20) and $\eta = 0$. There exist at most two local minima of $\tilde{\theta}$ on $[\psi_0, \pi]$. If the wedge angle $\psi_0 \geq \pi - \frac{\pi}{\sqrt{2}}$, then the local minimum is unique on $[\psi_0, \pi]$.*

Proof Depending on the choice of constants C_1 and C_2, the sign of $R(\psi)$ changes. Notice that $R(\psi)$ is a decreasing function on (ψ_0, π). Hence there may exists $\tau \in [\psi_0, \pi]$ such that $R(\psi) > 0$ for $\psi_0 < \psi < \tau$ and $R(\psi) < 0$ for $\tau < \psi < \pi$. If $\pi - \tau > \frac{\pi}{\sqrt{2}}$, then Lemma 1 implies that the solution blows up. Hence we may delete this case. Lemma 1 also implies that $\tilde{\theta}$ has no local minimum on (τ, π). Hence, if $\tau - \psi_0 < \frac{\pi}{\sqrt{2}}$, then there exists at most one local minimum in (ψ_0, τ) since the distance between two local minimum points should be larger than $\frac{\pi}{\sqrt{2}}$ by Lemma 2. If $\psi_0 \geq \pi - \frac{\pi}{\sqrt{2}}$, then, for any $0 \leq \tau \leq \pi$, $\tau - \psi_0 < \frac{\pi}{\sqrt{2}}$ and hence there is at most one local minimum. Furthermore, since $\frac{\pi}{2} < \frac{\pi}{\sqrt{2}}$, it is not possible to have three local minima even if $\tau = \pi$ and $\psi_0 = 0$. Hence, there are at most two local minima of $\tilde{\theta}$. □

Notice that our numerical simulations provide a unique local minimum on interval (ψ_0, π). We could only show the uniqueness of the local minimum for the case that $\psi_0 \geq \pi - \frac{\pi}{\sqrt{2}}$ and $\eta = 0$.

5 Concluding remarks: Maxwell's incomplete computation

In the introduction to this paper we have given a short description of Maxwell's derivation of what are now called the Burnett equations. Maxwell's computation was for only linear terms and in fact he only displays one of the three momentum equations (59) and his equations (as Maxwell noted correctly on p. 248) are missing the crucial shear stress. Hence it is natural to ask if Maxwell had included the shear stress would he have derived the experimentally observed motion? We see in the Korteweg theory the shear stress T_{12}^K is linear in $\hat{\rho}'$, say as given (3.6), and it seems likely Maxwell would have recovered this term as well. More striking however, since Maxwell was dealing with the Burnett equations, as we have shown in Section 1, his coefficient would would be the opposite sign of our $A > 0$. Hence, while Maxwell could have completed his calculation he would have found a new type of "Bobylev instability" 100 years before Bobylev's result, i.e., the gas would move but opposite to the experimentally observed direction.

6 Appendix

6.1 Finding appropriate similarity scales

In this section we briefly discuss how the scales in (4.4) have been obtained. To find a similarity solution in a form of

$$\begin{aligned} \rho &= r^{\alpha}\tilde{\rho}(\psi), \\ \theta &= r^{\beta}\tilde{\theta}(\psi), \\ w_1 &= r^{\gamma_1}\tilde{w}_1(\psi), \\ w_2 &= r^{\gamma_2}\tilde{w}_2(\psi), \\ T_{ij} &= r^{\delta}\tilde{T}_{ij}(\psi), \end{aligned} \tag{A.1}$$

we are looking for equations for $\tilde{\rho}, \tilde{\theta}, \tilde{w}_1, \tilde{w}_2$ and $\tilde{T}_{ij}$ with the angular variable "ψ" only. Our strategy is simple. If (i) each term in a balance law shares an identical power of r after a substitution of (A.1) into (1.1),(1.2) and hence (ii) the radial variable can be cancelled out after this substitution, then we may expect a self-similar solution.

For example, the two terms in the mass balance law are written as

$$\rho w_1 = r^{\alpha}\tilde{\rho} r^{\gamma_1}\tilde{w}_1, \quad \rho w_2 = r^{\alpha}\tilde{\rho} r^{\gamma_2}\tilde{w}_2.$$

Therefore, the first requirement is

$$\alpha + \gamma_1 = \alpha + \gamma_2, \tag{6.1}$$

which gives $\gamma_1 = \gamma_2 =: \gamma$.

For the isobaric case, the powers α and β should satisfy the isobaric relation

$$\alpha + \beta = 0,$$

and the elasticity contribution to the tensor T_{ij} disappears since the pressure p is constant. Now, there are three terms left in the momentum balance. The scales of these terms in radial direction are given in (4.7)–(4.9). These three scales give three equations

$$\begin{aligned} \alpha + 2\gamma &= \delta, \\ \beta\eta + \gamma - 1 &= \delta, \\ \beta(b-a-2) - 2 &= \delta. \end{aligned}$$

In this system, there are four unknowns, α, β, γ and δ, and four equations including the isobaric relation. Hence one may expect a unique similarity scale. Notice that the relation in (4.10) is simplified if $\delta = -1$. If we choose the Korteweg coefficient to be $c(\rho, \theta) = A\rho^a\theta^b$ with $b - a = 3 + 2\eta$, then we may have $\delta = -1$. The similarity scales of the case are the ones given in (4.4).

6.2 Maximum principle

In this section we introduce one dimensional maximum principle [32, Theorem 14 of Chap.1] used in this paper in a simplified version, which suffices for our situation. Let g and h be bounded and consider an operator

$$(L+h)[u] = u'' + g(x)u' + h(x)u.$$

Maximum principle: *Let $z_1(x)$, $z_2(x)$ and $w(x)$ be smooth functions on an interval $[a_1, a_2]$ with the following properties:*

1. $w > 0$ *on* $[a_1, a_2]$.
2. $z_1(a_1) \le z_2(a_1) = \gamma_1$ *and* $z_1'(a_1) \le z_2'(a_1) = \gamma_2$.
3. $z_1'(a_1)w(a_1) - z_1(a_1)w'(a_1) \le \gamma_2 w(a_1) - \gamma_1 w'(a_1) \le z_2'(a_1)w(a_1) - z_2(a_1)w'(a_1)$.
4. $(L+h)[w] \le 0$, $(L+h)[z_1] \le (L+h)[z_2]$.

Then,

$$z_1(x) \le z_2(x) \quad \textit{for} \quad a_1 \le x \le a_2.$$

This maximum principle has been used in the proof of Lemmas 1 and 2. For the proof of Lemma 1, we take $g(x) = 0$, $h(x) = 2$, $z_2(a_1) = z_1(a_1)$, $z_2'(a_1) = z_1'(a_1)$, and

$$w(x) = \sin(\sqrt{2}(\psi - a_1 + \epsilon)\,).$$

Then, we may apply the maximum principle on the domain $[a_1, a_1 + \frac{\pi - 2\epsilon}{\sqrt{2}}]$, where ϵ can be arbitrary small. For the proof of Lemma 2, we take $g(x) = 0$, $h(x) = 2 - \frac{2}{3}R(\psi)\tilde{\rho}$, $0 = z_2(a_1) = z_1(a_1)$, $0 \ge z_2'(a_1) \ge z_1'(a_1)$, and the same w. One can easily check that all assumptions in the theorem are satisfied.

Acknowledgements: Authors would like to thank Prof. Henning Struchtrup of the University of Victoria, British Columbia, Canada for his valuable remarks and help in the preparation of this paper. This work was done during

the third author's visit to Korea Mathematics Research Station (KMRS) of KAIST in Daejeon, Korea. He would like to thank all hospitality and support provided by the center during his stay. Y.J.Kim and M.Lee was supported in part by the National Research Foundation of Korea (grant numbers: 2011-0013447 and NRF-2007-0054245). M.Slemrod was supported in part by the Simons Foundation Collaborative Research Grant 232531.

References

1. A.V. Bobylev, *The Chapman-Enskog and grad methods for solving the Boltzmann equation*, Soviet Phys. Dokl. **27** (1982), 29–31.
2. ———, *Instabilities in the Chapman-Enskog expansion and hyperbolic Burnett equations*, J. Stat. Phys. **124** (2006), no. 2-4, 371–399. MR 2264613 (2007i:82066)
3. ———, *Generalized Burnett hydrodynamics*, J. Stat. Phys. **132** (2008), no. 3, 569–580. MR 2415120 (2009d:82123)
4. A.V. Bobylev and A. Windfäll, *Boltzmann equation and hydrodynamics at the Burnett level*, Kinet. Relat. Models **5** (2012), no. 2, 237–260. MR 2911095
5. D. Burnett, *The distribution of velocities in a slightly non-uniform gas*, Proc. London Math. Soc. **S2-39** (1935), no. 1, 385–430. MR 1576911
6. ———, *The distribution of molecular velocities and the mean motion in a non-uniform gas*, Proc. London Math. Soc. **S2-40** (1936), no. 1, 382–435. MR 1575832
7. C. Cercignani, *The Boltzmann equation and its applications*, Applied Mathematical Sciences, vol. 67, Springer-Verlag, New York, 1988. MR 1313028 (95i:82082)
8. S. Chapman and T.G. Cowling, *The mathematical theory of nonuniform gases*, third ed., Cambridge Mathematical Library, Cambridge University Press, Cambridge, 1990, An account of the kinetic theory of viscosity, thermal conduction and diffusion in gases, In co-operation with D. Burnett, With a foreword by Carlo Cercignani. MR 1148892 (92k:82001)
9. C.-C. Chen, I.-K. Chen, T.-P. Liu, and Y. Sone, *Thermal transpiration for the linearized Boltzmann equation*, Comm. Pure Appl. Math. **60** (2007), no. 2, 147–163. MR 2275326 (2007h:82074)
10. I.-K. Chen, *Boundary singularity of moments for the linearized boltzmann equation*, Journal of Statistical Physics **153** (2013), no. 1, 93–118 (English).
11. I.-K. Chen, H. Funagane, S. Takata, and T.-P. Liu, *Singularity of the velocity distribution function in molecular velocity space*, preprint (2014).
12. I-Kun Chen, Tai-Ping Liu, and Shigeru Takata, *Boundary singularity for thermal transpiration problem of the linearized Boltzmann equation*, Arch. Ration. Mech. Anal. **212** (2014), no. 2, 575–595. MR 3176352
13. C.M. Dafermos, *Hyperbolic conservation laws in continuum physics*, third ed., Grundlehren der Mathematischen Wissenschaften [Fundamental Principles of Mathematical Sciences], vol. 325, Springer-Verlag, Berlin, 2010. MR 2574377 (2011i:35150)
14. J.E. Dunn and J. Serrin, *On the thermomechanics of interstitial working*, Arch. Rational Mech. Anal. **88** (1985), no. 2, 95–133. MR 775366 (86f:73051)
15. Alexander N. Gorban and Ilya Karlin, *Hilbert's 6th problem: exact and approximate hydrodynamic manifolds for kinetic equations*, Bull. Amer. Math. Soc. (N.S.) **51** (2014), no. 2, 187–246. MR 3166040
16. A.N. Gorban and I.V. Karlin, *Structure and approximation of the Chapman-Enskog expansion for linearized Grad equations*, Soviet Phys. JETP **73** (1991), 637–641.
17. ———, *Structure and approximations of the Chapman-Enskog expansion for the linearized Grad equations*, Transport Theory Statist. Phys. **21** (1992), no. 1-2, 101–117. MR 1149364 (92m:82117)
18. ———, *Short wave limit of hydrodynamics: a soluble model*, Phys. Rev. Lett. **77** (1996), 282–285.
19. H. Grad, *On the kinetic theory of rarefied gases*, Comm. Pure Appl. Math. **2** (1949), 331–407. MR 0033674 (11,473a)

20. ———, *Principles of the kinetic theory of gases*, Handbuch der Physik (herausgegeben von S. Flügge), Bd. 12, Thermodynamik der Gase, Springer-Verlag, Berlin, 1958, pp. 205–294. MR 0135535 (24 #B1583)
21. I.V. Karlin and A.N. Gorban, *Hydrodynamics from Grad's equations: what can we learn from exact solutions?*, Ann. Phys. **11** (2002), no. 10-11, 783–833. MR 1957348 (2004e:82050)
22. I.V. Karlin, A.N. Gorban, G. Dukek, and T.F. Nonnenmacher, *Dynamic correction to moment approximations*, Physical Review E **57** (1998), no. 2, 1668–1672.
23. D.J. Korteweg, *Sur la forme que prennent les équations dumouvements des fluides si l'on tient compte des forces capillaires causes par des variations de densité*, Arch. Neerl. Sci. Exactes Nat. Ser. II **6** (1901), 1–24.
24. D.A. Lockerby, J.M. Reese, D.R. Emerson, and R.W. Barber, *Velocity boundary condition at solid walls in rarefied gas calculations*, Physical Review E **70** (2004), no. 1, 017303.
25. D.A. Lockerby, J.M. Reese, and M.A. Gallis, *The usefulness of higher-order constitutive relations for describing the Knudsen layer*, Physics of fluids **17** (2005), no. 10, 100609.
26. S.K. Loyalka and H. Ferziger, *Model dependence of the slip coefficient*, Phys. Fluids **10** (1967), 1833–1839.
27. S.K. Loyalka and K.A. Hickey, *Velocity slip and defect: hard sphere gas*, Phys. Fluids A (1989), 612–614.
28. S.K. Loyalka, N. Petrellis, and T.S. Storvick, *Some numerical results for the BGK model: thermal creep and viscous slip problems with arbitrary accommodation at the surface*, Phys. Fluids **18** (1975), 1094–1099.
29. J.C. Maxwell, *On stresses in rarefied gases arising from inequalities of temperature*, Phil. Trans. Roy. Soc. (London) **170** (1879), 231–256.
30. T. Ohwada, Y. Sone, and K. Aoki, *Numerical-analysis of the poiseuille and thermal transpiration flows between 2 parallel plates on the basis of the Boltzmann-equation for hard-sphere molecules*, Physics of fluids A-fluid dynamics **1** (1989), no. 12, 2042–2049.
31. ———, *Numerical-analysis of the shear and thermal creep flows of a rarefied-gas over a plane wall on the basis of the linearized Boltzmann-equation for hard-sphere molecules*, Physics of fluids A-fluid dynamics **1** (1989), no. 9, 1588–1599.
32. Murray H. Protter and Hans F. Weinberger, *Maximum principles in differential equations*, Springer-Verlag, New York, 1984, Corrected reprint of the 1967 original. MR 762825 (86f:35034)
33. L. Saint-Raymond, *A mathematical pde perspective on the Chapman-Enskog expansion*, Bull. Amer. Math. Soc. (N.S.).
34. ———, *From Boltzmann's kinetic theory to Euler's equations.*, Physica D **237** (2008), 2028–2036.
35. ———, *Hydrodynamic limits of the Boltzmann equation*, Lecture Notes in Mathematics, vol. 1971, Springer-Verlag, Berlin, Germany, 2009.
36. M. Slemrod, *Admissibility criteria for propagating phase boundaries in a van der Waals fluid*, Arch. Rational Mech. Anal. **81** (1983), no. 4, 301–315. MR 683192 (84a:76030)
37. M. Slemrod, *Dynamic phase transitions in a van der Waals fluid*, J. Differential Equations **52** (1984), no. 1, 1–23. MR 737959 (85e:76040)
38. M. Slemrod, *Chapman-Enskog $\Rightarrow$ viscosity-capillarity*, Quart. Appl. Math. **70** (2012), no. 3, 613–624. MR 2986137
39. ———, *Admissibility of weak solutions for the compressible Euler equations, $n \geq 2$*, Phil. Trans. R. Soc. A **371** (2013), no. 3, 1–11.
40. ———, *From Boltzmann to Euler: Hilbert's 6th problem revisited*, Comput. Math. Appl. **65** (2013), no. 10, 1497–1501. MR 3061719
41. Y. Sone, *Flows induced by temperature fields in a rarefied gas and their ghost effect on the behavior of a gas in the continuum limit*, Annual review of fluid mechanics, Vol. 32, Annu. Rev. Fluid Mech., vol. 32, Annual Reviews, Palo Alto, CA, 2000, pp. 779–811. MR 1744318 (2000k:76120)
42. Y. Sone and T. Doi, *Ghost effect of infinitesimal curvature in the plane Couette flow of a gas in the continuum limit*, Phys. Fluids **16** (2004), no. 4, 952–971. MR 2060764 (2005a:76141)

43. H. Struchtrup, *Macroscopic transport equations for rarefied gas flows*, Interaction of Mechanics and Mathematics, Springer, Berlin, 2005, Approximation methods in kinetic theory. MR 2287368 (2009f:76150)
44. H. Struchtrup and P. Taheri, *Macroscopic transport models for rarefied gas flows: a brief review*, IMA J. Appl. Math. **76** (2011), no. 5, 672–697. MR 2837614 (2012j:76083)
45. P. Taheri, A.S. Rana, M. Torrilhon, and H. Struchtrup, *Macroscopic description of steady and unsteady rarefaction effects in boundary value problems of gas dynamics*, Contin. Mech. Thermodyn. **21** (2009), no. 6, 423–443. MR 2576405 (2010k:76095)
46. S. Takata and H. Funagane, *Singular behaviour of a rarefied gas on a planar boundary*, J. Fluid Mech. **717** (2013), 30–47.
47. A. E. Tzavaras, *Plastic shearing of materials exhibiting strain hardening or strain softening*, Arch. Rational Mech. Anal. **94** (1986), no. 1, 39–58. MR 831769 (87e:73054)
48. ———, *Shearing of materials exhibiting thermal softening or temperature dependent viscosity*, Quart. Appl. Math. **44** (1986), no. 1, 1–12. MR 840438 (87m:76007)
49. ———, *Effect of thermal softening in shearing of strain-rate dependent materials*, Arch. Rational Mech. Anal. **99** (1987), no. 4, 349–374. MR 898715 (88i:73068)